International Journal of Adhesion & Adhesives 67 (2016) 69–75

Contents lists available at ScienceDirect

International Journal of Adhesion & Adhesives

journal homepage: www.elsevier.com/locate/ijadhadh

Influence of the engagement ratio on the shear strength of an epoxy adhesive by push-out tests on pin-and-collar joints: Part I: Campaign at room temperature

Dario Croccolo, Massimiliano De Agostinis, Stefano Fini, Giorgio Olmi *

Department of Industrial Engineering (DIN), University of Bologna, Viale del Risorgimento 2, 40136 Bologna, Italy

ARTICLE INFO

Available online 25 December 2015

Keywords:
Two-component epoxy adhesive
Engagement Ratio
Shear Strength
Pin-and-Collar Samples

ABSTRACT

This paper focuses on an epoxy adhesive (LOCTITE 9466), which is particularly suitable for applications involving different materials and where a clearance is present between the adherents. The investigated subject is concerned with the effect of the Engagement Ratio (*ER*, coupling length over coupling diameter) on the shear strength of LOCTITE 9466 at room temperature. Motivations arise from the increasing interest in epoxy-adhesive joints in lightweight structures and from the consequent need for design data. Decoupling tests have been performed on pin-and-collar samples manufactured according to current Standards. The height has been adjusted in order to explore a sufficiently wide *ER* range at four different levels. The results have been processed by the tools of the Analysis of Variance and of the Fisher test to investigate the significance or the not significance of *ER* on the joint shear strength. The final outcome was that *ER* significantly affects resistance at a very high confidence level. This result has then been refined by the tool of orthogonality, in order to allocate the differences among the four levels of *ER*. This further analysis has shown that the joint strength is significantly enhanced, when *ER* exceeds 1 and assumes values around 1.3 or higher.

1. Introduction

Adhesively bonded joints are used in many mechanical applications, because they offer several advantages, such as the reduction of weight, the increasing of strength and the improvement of fatigue and fretting corrosion. These advantages have been demonstrated to be effective in the case of interference fitted and adhesively bonded joints [1], namely, hybrid joints, whatever is the production system. Many researches evaluated the strength of these joints in dependence of several variables, such as the assembly pressure level [2], the type of materials in contact [3–4], the curing methodology [5], the operating temperature [6–7], the loading type [8–9] and type of joining technique [10–11]. In order to reduce the weight and the amount of the material, it is possible to reduce the Engagement Ratio (*ER*), which is the ratio between the coupling length over the coupling diameter. However, the reduction of the *ER* may lead to a reduction in the strength of the joint, therefore, its effect has been deeply investigated in a pin-and-collar set of specimens in the case of anaerobic adhesive [12].

The anaerobic adhesive is really effective in the case of metal parts to be connected and, particularly, in the case of steel components, whereas in the case of aluminium alloy or, worse, of composite material, the adhesive strength is strongly reduced [4]. A more suitable adhesive in such cases is the epoxy one that is, normally, used in slip-fit joints, where a clearance is present between the adherents. An additional and particularly relevant advantage of epoxy adhesives is that they offer the opportunity of bonding materials with different physical and mechanical properties, without triggering detrimental variations of their chemical structure. An important outcome is that epoxy adhesives can be successfully used to bond protective coatings to structural parts, thus achieving simple repair, with many applications in petroleum, aviation and aerospace industries [13–15]. A further application field is related to the development of joints between different materials, usually a steel shaft and a composite hub, mainly in automotive. According to [16], composites are the most suitable materials for many suspension components in racing cars, where lightweight properties are essential for successful race participation. Examples of parts that are better suited to composites are pushrods, A-arms and steering arms, due to the tensile/compressive load they experience in operation conditions and as an effect of their good response in terms of strength and stiffness. Similar design strategies are likely to be followed even in high class car

* Corresponding author. Tel.: +39 051 2093455; fax: +39 051 2093412.
E-mail address: giorgio.olmi@unibo.it (G. Olmi).

http://dx.doi.org/10.1016/j.ijadhadh.2015.12.028
0143-7496/

List of Symbols

A	Coupling surface [mm^2]
C	Number of columns (levels) in the ANOVA [-]
D_C	Coupling diameter [mm]
$F_{Ad.}$	Decoupling force [N]
$F_{calc.}$	Fisher's ratio [-]
L_C	Coupling length [mm]
$\tau_{Ad.}$	Adhesive static shear strength [MPa]
R	Number of rows (replications) in the ANOVA [-]

List of Acronyms

ANOVA	Analysis of Variance
ER	Engagement Ratio
LSD	Fisher's Least Significant Difference
MSQ	Mean Squares (general term)
MSBC	Mean Square Between Columns
MSW	Mean Square Within Columns
SSBC	Sum of Squares Between Columns
SSQ	Sum of Squares (general term)
SSW	Sum of Squares Within Columns
TSS	Total Sum of Squares
p-v.	*p*-value

mass production. Epoxy adhesives, like LOCTITE 9466, are generally used for bonding composite tubes with steel shafts, thus obtaining mixed material joints, whose strength is often difficult to predict. Consequently, there is an increasing need for design data, involving in particular the effect of the length of the joint: an increased length is indeed able to positively enhance the joint strength, but with the outcome of an overall increase in dimensions and weight. The lack of studies investigating the effect of *ER* inspired the present work, whose subject consists in the experimental investigation of the effect of *ER* on the shear strength of LOCTITE 9466 epoxy adhesive. Tests on pin-and-collar samples have been conducted at room temperature, with the cylindrical geometry of specimens being justified by the aforementioned applications in the automotive field.

2. Materials and methods

First of all, the specimens have been designed and produced, following the Standard ISO 10123 [17] for slip-fit joints. The sketch of the pin-and-collar samples produced and tested is reported in Fig. 1. Since the ISO 10123 suggests to choose an $ER=0.9$ and since the dimensions investigated in [12] are of four types (the half, the double and an intermediate value $ER=1.3$), the *ER*s values were set at the same value for this work. The collars have been designed, so that their diameters were consistent with the recommended values in [17–18]. Their heights have been adjusted, in order to meet the aforementioned values of *ER*, while the chamfer dimensions have been maintained unchanged, as well as the pin dimensions. The material of the samples is C40 UNI EN 10083-2 steel, whereas the adhesive type is the previously mentioned commercial LOCTITE® 9466, which is an epoxy glue with two components. In order to improve the statistical analysis and the definition of the significance of the *ER* parameter, a number of ten replications for each different *ER* has been chosen. The overall sample population consisted therefore of 40 Pin-and-collars for statistical evidence reasons. The whole set of specimens has been measured, in order to accurately determine the coupling diameters and to check their height values. For this purpose, a

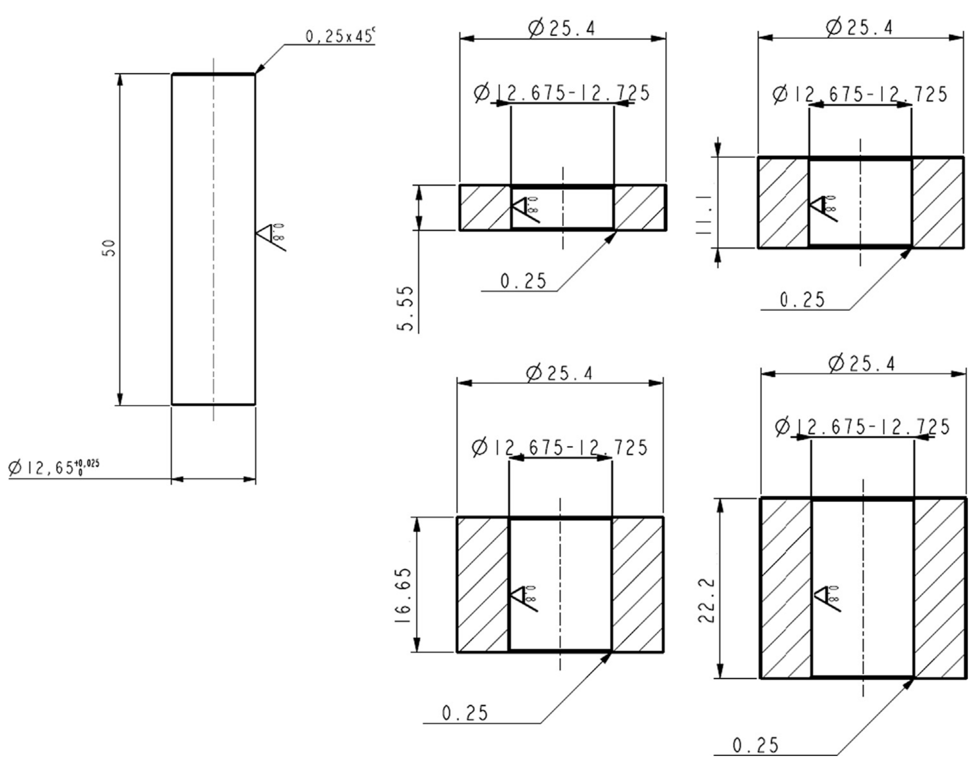

Fig. 1. Pin-and-collar specimens with $ER=0.4$ (a), $ER=0.9$ (b), $ER=1.3$ (c), $ER=1.7$ (d) (all dimensions in mm).

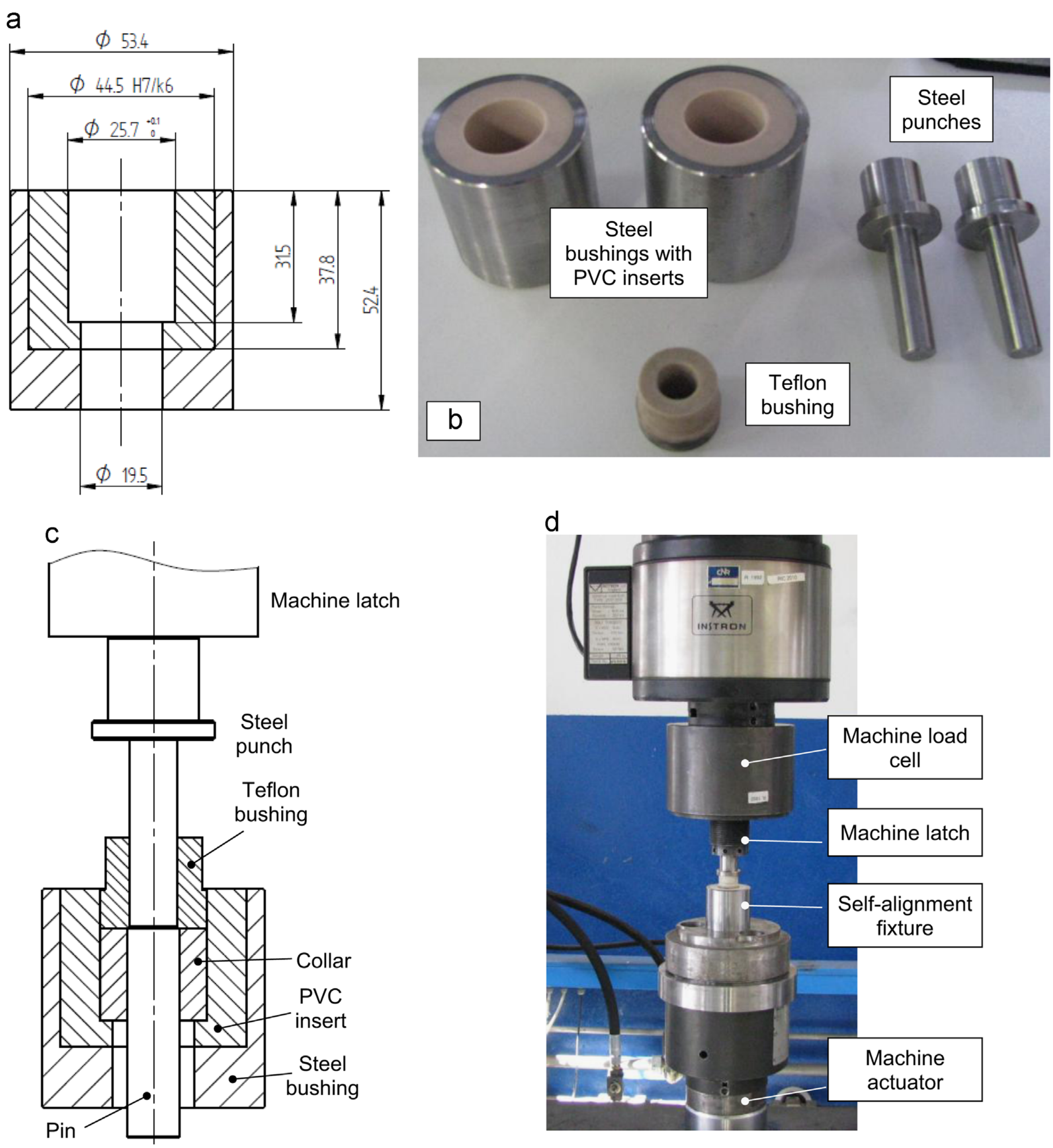

Fig. 2. (a) Drawing of the bushing with inner PVC insert (all dimensions in mm), (b) two sets of self-alignment device, experimental setting in trial conditions shown by a section view (c) and a picture taken just after decoupling (d).

micrometre screw gauge, an inside micrometre, and a digital caliper, all with the resolution of 0.01 mm, have been used.

An important issue regards misalignments, which could arise during the pushing-out phase and may seriously affect results. In order to overcome this point, a self-aligning rig has been specifically developed. It consists of a steel punch with a Teflon bushing for its alignment and of a fixture for the pin-and collar samples. This has been worked out as a component consisting of two parts: a steel bushing and a PVC insert, where the samples were intended to be placed just before the pushing-out procedure. The goal of the here described research was to perform an experimental campaign at room temperature; however, a key issue of the fixture design was that it could be suitable even to tests at incremented temperature, to be performed at a subsequent stage of the study. Using the same device for testing has been essential to ensure the consistency of results. This is the reason why a PVC internal bushing was used: taking advantage of its low thermal conductivity coefficient made it possible to reduce heat dissipation. A drawing of the bushing with inner PVC insert and a photo of two sets of self-alignment devices are shown in Fig. 2. The experimental setting is also shown in the same figure by a section view of the described rig after the insertion of a sample and by a photo taken just after specimen decoupling.

The decoupling tests have been performed by a standing press, where the pushing-out force, $F_{Ad.}$, was on-line measured. The shear strength $\tau_{Ad.}$ was finally computed as in Eq. (1), where A indicates the coupling area and D_c and L_c are the coupling diameter and length. D_c is computed as the average between the pin external diameter and the collar internal diameter. Finally, L_c is the collar length.

$$\tau_{Ad.} = \frac{F_{Ad.}}{A} = \frac{F_{Ad.}}{\pi \cdot D_c \cdot L_c} \tag{1}$$

Fig. 3. Pin and collar samples with the assembly tools.

3. Experimental procedure

It has been remarked that the coupling diameters of the pins and of the collars were carefully measured. It was the opportunity to sort them out, in order to suitable combine the two parts with the aim of maintaining the level of clearance at an approximately constant value. Proceeding this way, the clearance average was in the order of 60 µm with a standard deviation of 15 µm, thus meeting the requirements of [17–18].

The assembly procedure was the following for the whole set of specimens:

1. The surfaces were cleaned by the LOCTITE® 7063 cleaner and by a fine sandpaper;
2. The dual cartridge was inserted into the application gun and a light pressure was applied to the cylinders. The mixing nozzle provided by the manufacturer was mounted at the end of the cartridge to facilitate automatic mixing of resin and hardener. The two components were completely merged together, upon hand shaking for a few seconds until a uniform colour of the adhesive was obtained [19].
3. The adhesive was spread on the mating surfaces of the male and female parts and, just after, the collar was shifted over the pin, with a helicoidal back-and-forth rapid movement.
4. The exceeding glue was removed, as it could have affected the specimen length and therefore the *ER* related results.
5. The adhesive was cured for seven days at room temperature, as recommended in [19];

The samples collected before the joining operation and with the assembly tools described above, are reported in the picture of Fig. 3, whereas the joined specimens are reported in Fig. 4.

The push-out tests have been run by a standing press equipped by two load cells (connected in series), having capacities of 25 kN and 250 kN. All the trials have been run in displacement controlled conditions, applying a ramp with 0.03 mm/s speed, thus meeting the recommendations of [17]. This speed has been increased to 0.5 mm/s after the maximum peak of force ($F_{Ad.}$), to complete the decoupling. Both the applied force and the actuator displacement were recorded during the pushing-out procedure at the sampling rate of 30 Hz.

A further issue consisted in the possibility that the order of trials may somehow affect the experimental results in terms of the retrieved pushing-out force and of the resulting strength. This question has been overcome, using two identical self-aligning rigs (visible in Fig. 2), which have been alternatively mounted for decoupling tests, thus reducing the risk of their progressive deterioration. Moreover, the order of the tests involving the 40 samples with different *ER*s has been completely randomised, as suggested by Statistics Refs [20–21]. The tested specimens with the identification labels (#), pin and collar dimensions, clearances and *ER*s are reported in Table 1 in the actual randomised order followed in the experimental campaign. It can be observed that samples with different *ER*s are all mixed up in the sequence.

4. Results

An example of the pushing-out diagram acquired by the system, is shown in Fig. 5, with reference to a sample with $ER = 1.7$. The linear-elastic behaviour of the glue, the stick-slip phenomenon, which occurred in almost all the tested couplings, and the plastic part up to the complete separation of the two sample parts are highlighted in the graph. The static strength of the adhesive ($\tau_{Ad.}$) has been calculated, according to Eq. (1): the results, are reported in Table 2.

The adhesive strength values reported in Table 2 were then statistically analysed, in order to highlight if the *ER* parameter was significant.

5. Statistical analysis and discussion

As described in the previous Section, forty decoupling tests have been performed, involving pin-collar specimens, having four different *ER*s. Ten samples have been tested for each value of *ER*: the related results can be regarded as ten replications of the same measurement. The experimental outcomes, in terms of the shear strength of the adhesive, $\tau_{Ad.}$, are collected in Table 3, where the matrix columns correspond to the four levels of the *ER*, whereas the rows are related to the ten replicates *RN*. The results are also summarised in Fig. 6, where each of the four bars stands for the mean shear strength determined for each of the considered *ER*s.

The four means are computed as averages of the values in the four columns of Table 3. In order to have a full description of the experimental population, scatter bands, which account for the scattering from the minimum to the maximum values retrieved at each *ER* level, are added to each bar. As reported in the Introduction Section, one of the main goals of this research relies on the investigation of the effect of the *ER* on the adhesive response.

Especially from the point of view of structural design, it is important to discuss if the nominal adhesive strength may be affected, and, in case, enhanced, by a variation of the adherent length. The analysis of the bar graph in Fig. 6 suggests that the *ER* is likely to affect the adhesive response, since strength increases, as *ER* is incremented from 0.4 to 1.7. However, considering the related scatter bands, it can be easily observed that they are partially overlapped. Therefore, concluding that *ER* affects strength, would be questionable at this stage. In order to suitably tackle this question, the data in Table 3 have been processed by a one-factor Analysis of Variance (*ANOVA*) [20–21]. This approach makes it possible to compare the outputs for different values of the considered factor (*ER*), accounting also for the experimental uncertainty, i.e. for the scattering of the data. The adoption of this methodology is supported by its successful application in several references, e.g. [12, 22].

The output of the *ANOVA* is summarised in Table 4. The symbols in Table 4 have the meanings briefly described below, full details can be found in [20–21]. Considering initially the data in the first two columns, *SSQ* is a generic term for Sum of Squares. *SSBC* stands for the Sum of Squares Between Columns and has the meaning of the amount of the total variance, being related to the effect of the studied factor. It can be computed according to Eq. (2), where $\bar{y}_{.j}$ is the mean of the j-th column in Table 3 (i.e.: the mean strength for the j-th value of *ER*, plotted in Fig. 6) and $\bar{y}_{..}$ is the overall mean of the data in Table 3. Finally, *R* stands for the number of replications (ten in the present case), whereas *C* is the number of the considered levels for the factor *ER* (four).

$$SSBC = R \cdot \sum_{j=1}^{C} \left(\bar{y}_{.j} - \bar{y}_{..}\right)^2 \tag{2}$$

SSW is commonly regarded as the Sum of Squares Within (Columns) and is related to the amount of variance depending on

Fig. 4. Pin and collar samples assembled before the pushing-out operation.

Table 1
Test sequence and samples dimensions.

#	PIN	Diameter [mm]	COLLAR	Diameter [mm]	Length [mm]	Clearance [mm]	*ER*
1	A28	12.64	D41	12.67	16.69	0.03	1.32
2	A32	12.64	D40	12.67	16.69	0.03	1.32
3	A02	12.64	B24	12.67	16.7	0.03	1.32
4	C09	12.64	D25	12.68	16.67	0.04	1.31
5	C04	12.65	D05	12.69	5.6	0.04	0.44
6	C25	12.65	D21	12.69	16.67	0.04	1.31
7	A25	12.65	D22	12.69	16.66	0.04	1.31
8	A30	12.65	D02	12.71	5.63	0.06	0.44
9	C12	12.66	D12	12.71	11.09	0.05	0.87
10	C35	12.66	D10	12.72	5.65	0.06	0.44
11	C11	12.66	D39	12.72	11.09	0.06	0.87
12	C03	12.66	D11	12.72	11.1	0.06	0.87
13	C06	12.66	D17	12.72	11.14	0.06	0.88
14	C32	12.66	D07	12.72	5.63	0.06	0.44
15	C29	12.66	D38	12.72	11.08	0.06	0.87
16	C10	12.66	D09	12.71	5.58	0.05	0.44
17	C30	12.66	D14	12.72	11.1	0.06	0.87
18	C22	12.66	D19	12.72	11.07	0.06	0.87
19	C05	12.65	D08	12.71	5.65	0.06	0.44
20	C21	12.66	D15	12.72	11.13	0.06	0.88
21	C28	12.66	D20	12.72	11.11	0.06	0.87
22	C19	12.66	D18	12.72	11.1	0.06	0.87
23	C02	12.67	D03	12.73	5.57	0.06	0.44
24	C16	12.67	D29	12.73	16.67	0.06	1.31
25	C13	12.68	D23	12.73	16.71	0.05	1.31
26	C27	12.67	D04	12.73	5.62	0.06	0.44
27	C23	12.67	D06	12.73	5.59	0.06	0.44
28	E03	12.68	D28	12.76	16.68	0.08	1.31
29	A38	12.66	D26	12.8	16.77	0.14	1.31
30	C33	12.66	B41	12.745	22.22	0.085	1.74
31	C26	12.66	B42	12.74	22.21	0.080	1.74
32	C15	12.66	B43	12.745	22.21	0.085	1.74
33	E05	12.68	B44	12.745	22.24	0.065	1.74
34	A33	12.65	B31	12.675	22.23	0.025	1.75
35	A20	12.65	B40	12.68	22.25	0.03	1.75
36	A29	12.66	B33	12.68	22.5	0.02	1.77
37	A17	12.66	B34	12.68	22.24	0.02	1.75
38	C24	12.66	B35	12.68	22.24	0.02	1.75
39	C20	12.65	B37	12.68	22.25	0.03	1.75
40	C14	12.65	D01	12.71	5.59	0.06	0.44

Table 2
Test sequence and result values.

#	Load Cell capacity [kN]	$F_{Ad.}$ [kN]	A [mm^2]	$\tau_{Ad.}$ [MPa]
1	25	22	664.3	33.12
2	25	19.8	664.3	29.80
3	25	19.9	664.7	29.94
4	25	20.7	664.1	31.18
5	25	6.6	223.3	29.56
6	25	22.1	664.6	33.25
7	25	22.1	664.2	33.27
8	25	6.2	224.8	27.58
9	25	12.6	442.8	28.45
10	25	6.4	225.8	28.35
11	25	12	443.2	27.08
12	25	12.8	443.6	28.86
13	25	12.6	445.2	28.30
14	25	4.8	225.0	21.34
15	25	16.1	442.8	36.36
16	25	5.8	222.8	26.03
17	25	11.3	443.6	25.48
18	25	10.6	442.4	23.96
19	25	6.9	225.6	30.58
20	25	12.3	444.8	27.65
21	25	12.8	444.0	28.83
22	25	12.9	443.6	29.08
23	25	5.4	222.8	24.24
24	25	20.2	666.7	30.30
25	25	22.6	668.3	33.82
26	25	5.2	224.8	23.14
27	25	6.3	223.6	28.18
28	25	22.1	668.6	33.05
29	25	19.6	674.4	29.06
30	250	33.2	889.7	37.32
31	250	30.3	888.9	34.09
32	250	27.7	889.3	31.15
33	250	32.5	890.5	36.50
34	250	28.3	885.2	31.97
35	250	32.6	886.3	36.78
36	250	28.1	896.3	31.35
37	250	28.8	885.9	32.51
38	250	25.3	885.9	28.56
39	250	28.9	886.3	32.61
40	25	5.55	223.2	24.87

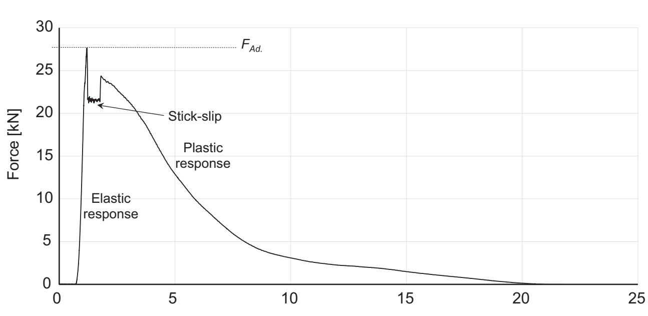

Fig. 5. Example of Force vs. Displacement diagram.

Table 3
Adhesive shear strengths $\tau_{Ad.}$: [MPa] determined for different *ERs*.

RN	*ER* = 0.4	*ER* = 0.9	*ER* = 1.3	*ER* = 1.7
1	29.6	28.5	33.1	37.3
2	27.6	27.1	29.8	34.1
3	28.3	28.9	29.9	31.1
4	21.3	28.3	31.2	36.5
5	26.0	36.4	33.3	32.0
6	30.6	25.5	33.3	36.8
7	24.2	24.0	30.3	31.4
8	23.1	27.7	33.8	32.5
9	28.2	28.8	33.1	28.6
10	24.9	29.1	29.1	32.6

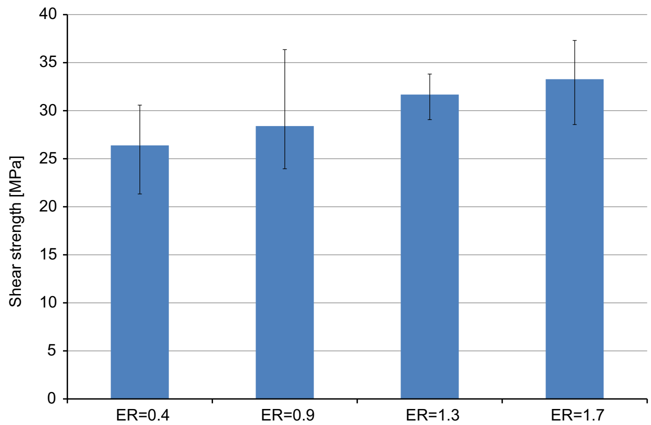

Fig. 6. Bar graph summarizing the mean values of $\tau_{Ad.}$ for different levels of *ER*, along with scatter bands.

Table 4
One-factor ANOVA to investigate the effect of *ER* on τ_{Ad}.

SSQ	*DoF*		*MSQ*		F_{calc}.	p-ν.
SSBC	291.72	3	MSBC	97.24	12.68	$8.29 \cdot 10^{-6}$
SSW	276.10	36	MSW	7.67		
TSS	567.82	39				

the uncertainty of the experiment. It is computed in Eq. (3), where y_{ij} is the yield in the i-th row and j-th column of Table 3.

$$SSW = \sum_{j=1}^{C} \left[\sum_{i=1}^{R} \left(y_{ij} - \bar{y}_{.j} \right)^2 \right] \quad (3)$$

TSS stands for the Total Sum of Squares and is the total amount of variance of the experiment. The latter is clearly related to the other terms by the following relationship: $TSS = SSBC + SSW$. The column referenced as *DoF* in Table 4 contains the degrees of freedom to be used to scale the *SSQs* and to finally retrieve the Mean Squares, generally indicated as *MSQ*. The Mean Square Between Columns (*MSBC*) and the Mean Square Within (Columns) (*MSW*) can be easily computed, dividing the *SSQs* by the corresponding degrees of freedom. The $F_{calc.}$ is then determined as a ratio between *MSBC* and *MSW* and has the meaning of the Calculated Fisher's ratio, to be used in the statistical Fisher's test. Finally, the p-ν. is usually regarded as the p-value and retains the meaning of the probability of failing, when stating that the factor does affect the output. This coefficient can be easily computed by electronic sheets, based on the Fisher's distribution. The resulting p-ν. is here very low, in the order of 10^{-6}, which indicates that there is a strong evidence that the *ER* has a significant influence on the adhesive strength $\tau_{Ad.}$.

This result indicates that significant differences are present between the yields in the columns of Table 3, obtained for different *ER*s. However, a possible drawback of the performed analysis is that it is not possible to directly allocate these differences. In other words, it is not possible to establish if the considered factor has an effect over the entire range, or if it is initially ineffective and acquires a significant impact only beyond a certain threshold of *ER*. The easiest option to tackle this question is to make use of a multiple-comparison test, to compare pairs of column means. Therefore, the Fisher's Least Significant Difference (*LSD*) test [20–21] has been used to compare the strengths determined for adjacent levels of *ER*. In particular, the strength for $ER = 0.4$ has been, initially, compared with the strength for $ER = 0.9$, while the further pairwise comparisons have involved level $ER = 0.9$ vs. level $ER = 1.3$ and level $ER = 1.3$ vs. level $ER = 1.7$. The application of the *LSD* criterion requires first the computation of the Least Significant Difference term that gives the name to the test. Its calculation, based on [20–21], and considering a 95% confidence level, has yielded the threshold value of 2.51, to be compared to differences of mean pairs.

Table 5
LSD Tests to investigate the significance of the differences between adjacent *ER* levels.

Test	Difference between means	*LSD* (Threshold)
$ER = 0.4$ vs. $ER = 0.9$	$\bar{y}.2 - \bar{y}.1 = 2.02$	
$ER = 0.9$ vs. $ER = 1.3$	$\bar{y}.3 - \bar{y}.2 = 3.27$	2.51
$ER = 1.3$ vs. $ER = 1.7$	$\bar{y}.4 - \bar{y}.3 = 1.60$	

Table 6
Augmented *ANOVA* to deepen the analysis of the effect of *ER* on $\tau_{Ad.}$.

SSQ		*DoF*	*MSQ*	$F_{calc.}$	*p-v.*
SSBC	291.72	3			
ER = 0.4 vs. ER = 0.9	*20.38*	*1*	*20.38*	*2.66*	*11.18%*
ER = 1.3 vs. ER = 1.7	*12.85*	*1*	*12.85*	*1.68*	*20.38%*
Low levels vs. High levels	*258.50*	*1*	*258.50*	*33.70*	$1.3 \cdot 10^{-6}$
SSW	276.10	36	7.67		
TSS	567.82	39			

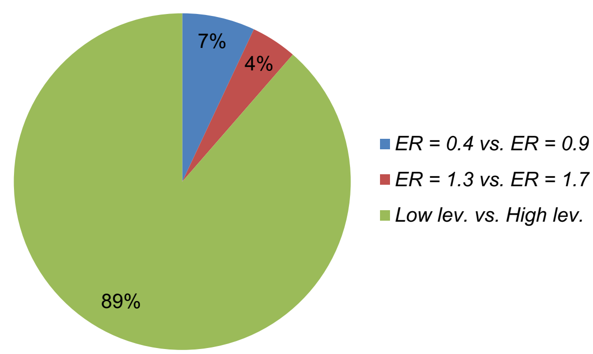

Fig. 7. Partition of the *SSBC*.

A resume of the results is shown in Table 5, where the *LSD* threshold is computed for a 95% confidence level of each pairwise test.

The differences are significant, when they overcome the *LSD* threshold. Therefore, the difference between the results for $ER = 0.9$ and $ER = 1.3$ is significant (at the 95% confidence level). The conclusion of the multiple comparison tests is that significance differences do exist between the second and the third level of *ER*. In other words, there is a significant enhancement between the adhesive response at low levels (0.4, 0.9) of *ER* and that at high levels (1.3, 1.7). Following this result, the analysis has been deepened, according to the approach of the orthogonal decomposition of the *SSBC* [20, 22]. This approach makes it possible to split the *SSBC* into three terms, which account for the possible sources of variability, finally determining whether they are significant or not. In the present case, the *SSBC* has been divided into:

1. One term depending on the differences of $\tau_{Ad.}$ at low levels (0.4, 0.9) of *ER*;
2. A second term related to the differences of $\tau_{Ad.}$: at high levels (1.3, 1.7) of *ER*;
3. A third final term depending on the differences between the average response at low levels of *ER* (results for $ER = 0.4$ and $ER = 0.9$ taken together) and the average response at high levels (results for $ER = 1.3$ and $ER = 1.7$ together).

The results are reported in the augmented *ANOVA* in Table 6.

The outputs of the Fisher tests indicate that the first and second terms are not significant at the 5% significance level. This threshold is usually the most suitable, according to several references, e.g. [20–21]. Whereas, the amount of variance related to the different response of the adhesive at low and high values of the *ER* is highly significant (probability of error, when accepting the significance hypothesis in the order of 10^{-6}). This outcome is consistent with those of the *LSD* comparison tests and is confirmed by the graphical sketch of the *SSBC* partition, shown in the cake diagram in Fig. 7. It can be remarked that almost 90% of the total amount of the *SSBC* is due the incremented strength when using high *ER*s.

6. Conclusions

The present paper provides some preliminary information concerning the influence of the Engagement Ratio on the strength of epoxy adhesive with two components, the commercial LOCTITE® 9466. The specimens are the standard pin-and-collar samples, specifically adapted in order to change their original Engagement Ratio. Four different Engagement Ratios have been studied; one is equal to the original dimension, one is smaller and two are greater. The results have been statistically analysed in order to highlight the significance of the Engagement Ratio parameter. The present analysis pointed out a strong dependence of the adhesive strength on the Engagement Ratio value, even if the significance is restricted between the two low and the two high levels. In conclusion, a threshold limit for the Engagement Ratio value, seems to be set equal to 1, so that it is advisable to use values at least equal to 1.3-1.5.

References

[1] Croccolo D, De Agostinis M, Vincenzi N. Design and optimization of shaft-hub hybrid joints for lightweight structures: Analytical definition of normalizing parameters. Int J Mech Sci 2012;56(1):77–85.

[2] Dragoni E, Mauri P. Intrinsic static strength of friction interfaces augmented with anaerobic adhesives. Int J Adhes Adhes 2000;20(4):315–21.

[3] Sekercioglu T. Shear strength estimation of adhesively bonded cylindrical components under static loading using the genetic algorithm approach. Intl J Adhes Adhes 2005;25:352–7.

[4] Croccolo D, De Agostinis M, Vincenzi N. Design of hybrid steel-composite interference fitted and adhesively bonded connections. Int J Adhes Adhes 2012;37:19–25 Special Issue on Joint Design 3.

[5] Mengel R, Haberle J, Schlimmer M. Mechanical properties of hub/shaft joints adhesively bonded and cured under hydrostatic pressure. Intl J Adhes Adhes 2007;27:568–73.

[6] Da Silva LFM, Adams RD. Joint strength predictions for adhesive joints to be used over a wide temperature range. Intl J Adhes Adhes 2007;27:362–79.

[7] Da Silva LFM, Adams RD. Adhesive joints at high and low temperatures using similar and dissimilar adherends and dual adhesives. Int J Adhes Adhes 2007;27(3):216–26.

[8] Adams J, Comyn RD, Wake WC. Structural adhesive joints in engineering. London: Chapman & Hall; 1997.

[9] Croccolo D, De Agostinis M, Vincenzi N. Static and dynamic strength evaluation of interference fit and adhesively bonded cylindrical joints. Intl J Adhes Adhes 2010;30:359–66.

[10] Croccolo D, De Agostinis M, Mauri P. Influence of the assembly process on the shear strength of shaft-hub hybrid joints. Intl J Adhes Adhes 2013;44:174–9.

[11] Castagnetti D, Dragoni E. Experimental Assessment of a Micro-Mechanical Model for the Static Strength of Hybrid Friction-Bonded Interfaces. J Adhes 2013;89(8):642–59.

[12] Croccolo D, De Agostinis M, Mauri P, Olmi G. Influence of the engagement ratio on the joint strength of press fitted and adhesively bonded specimens. Int J Adhes Adhes 2014;53:80–8.

[13] Périchaud MG, Delétage JY, Frémont H, Danto Y, Faure C. Reliability evaluation of adhesive bonded SMT components in industrial applications. Microelectron Reliab 2000;40:1227–34.

[14] White KL, Sue H-J. Electrical conductivity and fracture behavior of epoxy/polyamide-12/multiwalled carbon nanotube composites. Polym Eng Sci 2011;51(11):2245–53.

[15] Warren GL, Sun L, Hadjiev VG, Davis D, Lagoudas D, Sue H-J. B-staged epoxy/single-walled carbon nanotube nanocomposite thin films for composite reinforcement. J Appl Polym Sci 2009;112:290–8.

[16] Olsen R., Bookholt A., Melchiori E. Composite Suspension for Formula SAE Vehicle, Senior Project presented to the Faculty of the Mechanical Engineering Department, California Polytechnic State University, San Luis Obispo, United States.

[17] ISO 10123. Adhesives-Determination of Shear Strength of Anaerobic Adhesives Using Pin-and-Collar Specimens; 1990.

[18] ASTM D4562-01. Standard Test Method for Shear Strength of Adhesives Using Pin-and-Collar Specimen; 2013.

[19] Henkel Web Site: ⟨http://tds.henkel.com/tds5/docs/EA%209466-EN.PDF⟩.

[20] Berger PD, Maurer RE. Experimental design with applications in management, engineering and the sciences. Belmont, CA: Duxbury Press; 2002.

[21] Montgomery DC. Design and analysis of Eeperiments. New York: Wiley; 2001.

[22] Olmi G. Investigation on the influence of temperature variation on the response of miniaturised piezoresistive sensors. Strain 2009;45:63–76.